AN INVERSION METHOD FOR ACOUSTIC WAVE FIELDS

Robert W. Clayton and Robert H. Stolt

Abstract

A method is derived for determining density and bulk-modulus variations in the earth from standard reflection surveys. Explicit formulas are given for the variations that utilize the amplitude information present in the observed wave fields. The method is based on a Born approximation of the scattering equation, and is consequently restricted to sub-critical reflections. The computations are done in the Fourier domain, where the first part of the algorithm is very similar to an F-K migration. The computational expense of the method is only slightly greater than that of F-K migration itself.

I. Introduction

In this paper we present a method for determining the bulk modulus and density variations of an acoustic medium from reflection data recorded along a horizontal datum. The field experiment necessary to provide the data for the method is a standard reflection survey with multiple offset coverage.

In reflection data, there are basically two sources of information about the subsurface: traveltimes and amplitudes. The traveltimes of the various wavefronts in the wave field provide information about the low spatial frequency components (trends) of the the medium parameters. For example, the velocity determined from NMO curves is a low-frequency average of the true velocity of the medium. The amplitudes of the wavefronts, on the other hand, are sensitive to the high spatial frequency components (the reflectors). Thus, the two types of information sample different aspects of the medium. In

this paper, we will be using the amplitude variations to determine the fine scale variations in the density and modulus.

The basic approach which we will be taking is to use a Born approximation of the Lippman-Schwinger equation, to develop a forward equation relating the surface data to a scattering potential. The scattering potential is an operator which depends on the medium parameters, and essentially represents the reflectivity of the medium. The highly structured form of the scattering potential for the acoustic problem will allow the forward equation to be inverted analytically. Thus, we will derive explicit formulas for the density and modulus variations as functions of the surface data.

The use of the Born approximation will entail several assumptions about the nature of the medium. Basically, the modulus and density variations must be small and localized (free of trends). Also, the method, as presented here, has no provisions for handling multiples or transmission effects, and is restricted to sub-critical reflections.

We will assume the source used in the experiment is band-limited. This usually causes problems with inversion methods because at some point in the inversion scheme, the source has to be deconvolved. This, of course, can be successfully done only within a limited passband, and attempts to invert data outside this passband will usually cause instabilities. We will bypass this problem by only reconstructing the parameter variations within a limited spatial frequency range.

II. The Born Approximation for the Scalar Wave Equation

In this section we will give a brief derivation of the Lippman-Schwinger equation for acoustic problems. The Born approximation of this equation will lead to a simple relation between the observations and the scattering potential.

The starting point of the derivation is the acoustic wave equation for a linear isotropic medium

$$L\,P = \left[\frac{\omega^2}{K} + \nabla\cdot\frac{1}{\rho}\nabla\right]P = 0 \qquad (1)$$

where P is the pressure field, K is the bulk modulus, and ρ is the density. Associated with the wave operator (L) is the Green's operator or resolvent which is formally defined as (Taylor, p. 129)

$$G = -L^{-1} \tag{2}$$

The Green's operator produces the response of the medium at one point due to an impulse at another. The knowledge of the Green's operator for a particular problem completely specifies the solutions for that problem.

In general, we cannot analytically determine solutions for equation (1) for arbitrary variations in ρ and K. Instead, solutions are usually cast as a perturbation about a simpler problem for which analytic solutions are available. In this paper we will perturb the Green's operator, and the problem which we will perturb about, is the one for which the wave operator is

$$L_o = \left[\frac{\omega^2}{K_o} + \nabla \cdot \frac{1}{\rho_o} \nabla\right] = \left[\frac{\omega^2}{K_o} + \frac{1}{\rho_o} \nabla^2\right] \tag{3}$$

where K_o and ρ_o are constants.

To relate G and G_o (the Green's operator for L_o), we employ the simple identity

$$A = B + B\,(B^{-1} - A^{-1})\,A$$

and associate G with A and G_o with B. Hence,

$$G = G_o + G_o\,V\,G \tag{4}$$

where $V = L - L_o$. Equation (4) is the Lippman-Schwinger equation for G, and V is termed the scattering potential. As written, equation (4) is implicit in G, but it can be formally solved

$$G = (I - G_o V)^{-1}\,G_o \tag{5}$$

The Born series is an expansion of the right-hand side of equation (5), in powers of the operator VG_o. The series can be generated by recursively substituting G for itself in the Lippman-Schwinger equation.

$$G = G_o + G_o VG$$

$$G = G_o + G_o V(G_o + G_o VG)$$

$$G = G_o + G_o VG_o + G_o VG_o V(G_o + G_o VG)$$

Rewriting this in sequence terms of powers of the operator VG_o, we have the Born series for G

$$G = G_o + G_o \sum_{i=1}^{\infty} (VG_o)^i \tag{6}$$

The Born approximation of the Lippman-Schwinger equation is the first two terms of the series.

$$G = G_o + G_o VG_o \tag{7}$$

In Dirac notation the Born approximation is[1]

$$\langle x_g|G|x_s\rangle = \langle x_g|G_o|x_s\rangle + \langle x_g|G_o|x''\rangle \langle x''|V|x'\rangle \langle x'|G_o|x_s\rangle \tag{8}$$

where x_s is the location of the source, and x_g is the observation point. When the velocity deviations of the medium are localized (i.e. there are no trends), the various terms in equation (8) may be physically interpreted with the aid of the Feynmann diagram shown in figure 1.

---

[1] In this paper, repeated dummy variables will generally signify an implied integration. For example, the second term in equation (8) is really an integral over the intermediate points x' and x''.

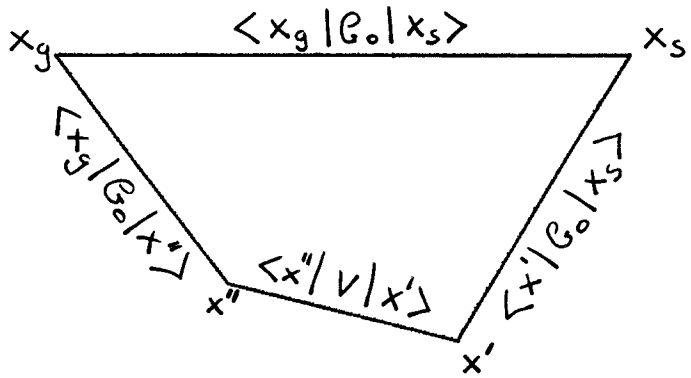

FIG. 1. The Feynmann diagram for interpreting the Born approximation. The operator $\langle x_g | G_o | x_s \rangle$ represents the direct wave from the source point x_s to the receiver point x_g. The operator $\langle x' | G_o | x_s \rangle$ determines the wave field at a subsurface point x'. The wave field is then scattered (reflected) by the scattering potential V, and evaluated at the subsurface point x''. The final operator $\langle x_g | G_o | x'' \rangle$ determines the wave field over the path from x'' to the receiver point x_g. The total response at the receiver is the integration over all subsurface points x' and x''.

The suitability of the Born approximation depends on the size and nature of the scattering potential V. There are basically two restrictions. First of all, since the Born approximation is obtained from a series expansion, it is necessary that the norm of V be small in order that the remaining terms can be neglected. Secondly, the variations in V should be local, that is V should not have trends in it. The necessity of this restriction is obvious, if we examine the behavior of the direct wave. Under the Born approximation, the traveltime of the direct wave is based on a constant velocity. If, however, there is a trend in velocity from the source to the receiver, the traveltime will be incorrect by an amount that gets progressively worse with larger offsets. If the above two assumptions about the scattering potential are valid, then the terms omitted in the Born approximation can be interpreted as transmission and multiple reflections.

For the acoustic problem, the scattering potential is simply the difference of the wave operators in equations (1) and (3).

$$V = \omega^2 \left(\frac{1}{K} - \frac{1}{K_o} \right) + \nabla \cdot \left(\frac{1}{\rho} - \frac{1}{\rho_o} \right) \nabla \qquad (9)$$

For convenience, we will define the dimensionless functions

$$a = \left[\frac{K_o}{K} - 1\right] \quad \text{and} \quad b = \left[\frac{\rho_o}{\rho} - 1\right]$$

and hence the scattering potential becomes

$$V = \omega^2 \frac{a}{K_o} + \nabla \cdot \frac{b}{\rho_o} \nabla \tag{10}$$

For the inverse problem, we will concentrate on finding the functions $a(x,z)$ and $b(x,z)$, and not worry about reconstructing the actually density and modulus variations from them.

The observations of the reflected wave field are made on the horizontal surface ($z_s = z_g = 0$). They are functions x_g, x_s, and ω. Using the Born approximation, the observed reflected wave field is related to the scattering potential by

$$\Psi(x_g, x_s, \omega) = \langle x_g, 0 | G_o | x', z' \rangle \langle x', z' | V | x'', z'' \rangle \langle x'', z'' | G_o | x_s, 0 \rangle \, S(\omega) \tag{11}$$

where $S(\omega)$ is the Fourier transform of the source time function. In this paper we are not including the effect of a free surface. We will, however, stop the medium above the datum from scattering by assuming that $a(x,z)$ and $b(x,z)$ are zero for $z < 0$.

Equation (11) is a forward equation in the sense that, given the density and modulus variations (a and b), the observed wave field can be computed. The remainder of the paper will be concerned with the inverse problem: finding a and b from measurements of Ψ. The first step is to find the Green's operator for the homogeneous problem, and this is done in Appendix A. The next step is to examine equation (11) in the Fourier domain.

III. The Scattering Equation in the Fourier Domain

We will now use the fact that the Green's operator in the (ω,k_x,z)-domain looks very much like the kernel of a Fourier transform to obtain a simple equation relating the observed data and the scattering potential.

Fourier transforming equation (11) over x_g and x_s, we obtain an expression for Ψ in the (k_g,k_s,ω)-domain.

$$\Psi(k_g,k_s,\omega) = \langle k_x|x_g\rangle \langle x_g,0|G_o|x',z'\rangle$$

$$\cdot \langle x',z'|V|x'',z''\rangle \langle x'',z''|G_o|x_s,0\rangle \langle x_s|k_s\rangle S(\omega) \qquad (12)$$

Substituting in directly from equations (A5) and (A6) we have

$$\Psi(k_g,k_s,\omega) = \frac{1}{2\pi}\int dx'\int dz'\int dx''\int dz'' \quad i\rho_o \frac{e^{i(k_g x' - \nu_g|z'|)}}{-2\nu_g}$$

$$\cdot V(x',z'|x'',z'') \quad i\rho_o \frac{e^{-i(k_s x'' + \nu_s|z''|)}}{-2\nu_s} S(\omega) \qquad (13)$$

where

$$\nu_g = \left(\frac{\omega^2}{v^2} - k_g^2\right)^{\frac{1}{2}} \quad \text{and} \quad \nu_s = \left(\frac{\omega^2}{v^2} - k_s^2\right)^{\frac{1}{2}}$$

At the outset, we assumed that both $a(x,z)$ and $b(x,z)$ are zero for $z < 0$. This means that we can drop the absolute signs in equation (13) because $V(x',z'|x'',z'')$ will be zero for either $z' < 0$ or $z'' < 0$. Equation (13) can now be recognized as a four-fold Fourier transform of the scattering potential over the variables x', z', x'', and z''. Thus, we obtain a very simple relationship between observed wave field and the scattering potential.

$$\Psi(k_g,k_s,\omega) = -\frac{2\pi\rho_o^2}{4\nu_s\nu_g} V(k_g,-\nu_g|k_s,\nu_s)\cdot S(\omega) \qquad (14)$$

In general, V is a function of four variables. However, from equation (14), one can see that the surface data depends only on the values of V on a shell or hyper-surface in the four-dimensional space. This is referred to in scattering theory as the "on-shell" part of the scattering potential. At first glance this would seem to make the inverse problem of finding the scattering potential from the observations under-determined. However, for the scalar wave equation, V has a highly structured form as is shown in Appendix B. This will allow the inverse problem to be solved.

IV. Inversion of the Scattering Equation

We can now do the final step of relating the surface data to a and b in the Fourier domain. From Appendix B, the Fourier transform of the scattering potential is

$$V(k'|k'') = \frac{1}{(2\pi)^2}\left[\omega^2 \frac{a(k'-k'')}{K_o} - k'\cdot k'' \frac{b(k'-k'')}{\rho_o}\right] \tag{15}$$

Combining equations (14) and (15) we have

$$\Psi(k_g,k_s,\omega) = \frac{-1}{2\pi}\frac{\rho_o^2\omega^2}{4\nu_g\nu_s}\left[\frac{1}{K_o}a(k_g-k_s,-\nu_g-\nu_s) + \frac{(\nu_g\nu_s - k_g k_s)}{\omega^2}\frac{1}{\rho_o}b(k_g-k_s,-\nu_g-\nu_s)\right]S(\omega) \tag{16}$$

The inverse problem is to find the functions a (the bulk-modulus variations) and b (the density variations) from the surface data Ψ. Since a and b depend on $k_g - k_s$ we will start by changing to midpoint-offset coordinates. The midpoint wavenumber (k_m) and half-offset wavenumber (k_h) are defined by[2]

[2]These definitions of midpoint and offset wavenumber differ from previous SEP reports. The difference arises because we have used a conjugate rather than a symmetric relationship between source and receiver. This follows directly from the Dirac notation. If the reader has any doubts, he can change equation (11) into midpoint-offset variables, then do a double Fourier transform and compare with equation (16).

$$k_m = k_g - k_s \quad \text{and} \quad k_h = k_g + k_s \tag{17}$$

Also since a and b depend on $\nu_g + \nu_s$ a new independent variable (k_z) is defined

$$k_z = -\nu_g - \nu_s = -\left(\frac{\omega^2}{v^2} - k_g^2\right)^{\frac{1}{2}} - \left(\frac{\omega^2}{v^2} - k_s^2\right)^{\frac{1}{2}} \tag{18}$$

After a little algebra, equations (18) and (19) may be combined to obtain expressions for ω, ν_g, and ν_s.

$$\omega = \frac{v}{2} k_z \left[\left(1 + k_m^2/k_z^2\right)\left(1 + k_h^2/k_z^2\right)\right]^{\frac{1}{2}} \equiv \omega(k_m, k_h, k_z) \tag{19}$$

$$\nu_g = \frac{k_z}{2}\left(1 - k_m k_h / k_z^2\right) \tag{20}$$

$$\nu_s = \frac{k_z}{2}\left(1 + k_m k_h / k_z^2\right) \tag{21}$$

To complete the coordinate transformation, a new dependent variable R, is defined

$$R(k_m, k_h, k_z) = \frac{2\pi}{\rho_o} \frac{\Psi[k_m, k_h, \omega(k_m, k_h, k_z)]}{S[\omega(k_m, k_h, k_z)]}. \tag{22}$$

Equation (22) is really the F-K migration of the surface data in midpoint-offset coordinates (Stolt, 1978). The result of migration is usually considered to be an image of the reflection coefficients in the earth, so one may view R as a reflectivity function. The problems associated with S in the denominator of equation (23) will be discussed in a moment. First, we will relate R to a and b.

Using the relationship between Ψ, a, and b given by equation (16), and the coordinate transformations of equations (17) and (18), we can obtain an equation for R in terms of a and b.

$$R(k_m,k_h,k_z) = C_1(k_m,k_h,k_z)\left[a(k_m,k_z) + C_2(k_h,k_z)\ b(k_m,k_z)\right] \tag{23}$$

where

$$C_1(k_m,k_h,k_z) = -\frac{1}{4}\frac{k_m^2 + k_z^2 + k_h^2\left[1 + k_m^2/k_z^2\right]}{k_z^2 - k_m^2k_h^2/k_z^2} \tag{24}$$

and

$$C_2(k_h,k_z) = \frac{k_z^2 - k_h^2}{k_z^2 + k_h^2} \tag{25}$$

To separate a and b in equation (23) we define the function

$$R'(k_m,k_h,k_z) \equiv \frac{R(k_m,k_h,k_z)}{C_1(k_m,k_h,k_z)} \tag{26}$$

R' is regular everywhere except at the origin ($k_m=k_h=k_z=0$). A comparison of R' at any two offset wavenumbers will yield a separation of $a(k_m,k_z)$ and $b(k_m,k_z)$. A more robust method of achieving the separation would be to minimize the square error

$$\left[R'(k_m,k_h,k_z) - a(k_m,k_z) - C_2(k_h,k_z)\ b(k_m,k_z)\right]^2 \tag{27}$$

A solution which does this is

$$a(k_m,k_z) = \frac{\Sigma C_2^2\cdot\Sigma R' - \Sigma C_2R'\cdot\Sigma C_2}{N\cdot\Sigma C_2^2 - \Sigma C_2\cdot\Sigma C_2} \tag{28}$$

and

$$b(k_m,k_z) = \frac{N\cdot\Sigma C_2R' - \Sigma R'\cdot\Sigma C_2}{N\cdot\Sigma C_2^2 - \Sigma C_2\cdot\Sigma C_2} \tag{29}$$

where the summations are over offset wavenumber, and N is the number of offset wavenumbers. N is actually a function of k_m and k_h. Care must be taken to average only over k_h points where data exists. This point will discussed further in the section on implementation.

The appearance of $S(\omega)$ in the denominator of equation (22) will be a source of trouble, if we try to implement the inversion directly, because the source we have assumed has a finite bandwidth $\Delta\omega(k_m,k_h,k_z)$. Attempts to find a and b outside this region will be unstable. One can ignore the source all together if one is willing to live with the fact that all discontinuities in a and b will have source wavelets attached to them. A more reasonable approach would be to deconvolve the source as well as possible within the passband, and set a and b to zero outside the passband. This will define a finite region in which $a(k_m,k_z)$ and $b(k_m,k_z)$ can be determined. The shaded portion of figure 2 shows this region for $k_h = 0$. For larger k_h it is in theory possible to partially fill in the missing hole in the middle, as indicated by equation (19).

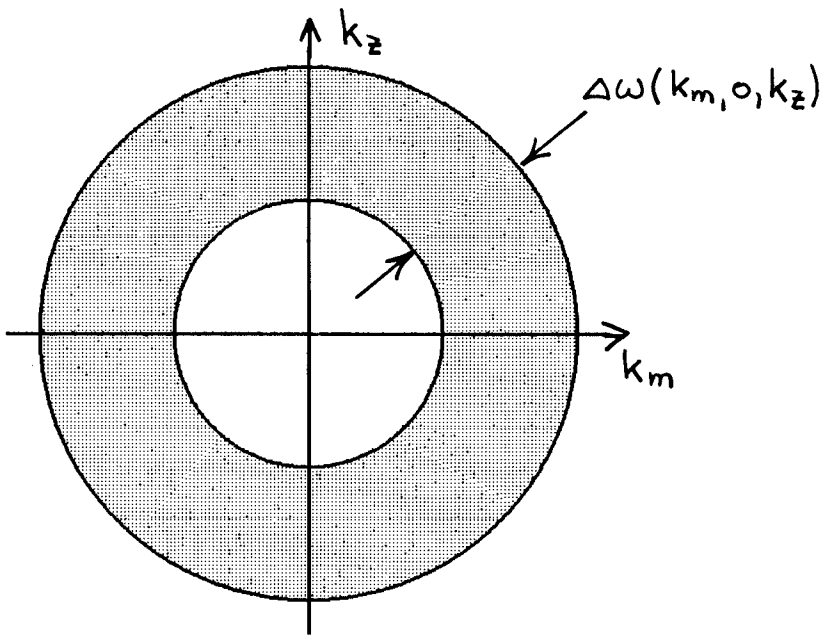

FIG. 2. The shaded portion shows the region in which the density and modulus can be successfully inverted. By using increasingly higher wavenumbers, it is in theory possible to fill in the hole in the center.

V. A Check On The Scalar Scattering Equation

To verify that the separation between density and modulus obtained in the previous section is not an artifact of the Born approximation, we will re-derive equation (23) for a simple case. The case we consider is that of a single horizontal reflector. In this case only $k_m = 0$ contributes, and consequently the coefficients C_1 and C_2 are

$$C_1 = -\frac{1}{4}\frac{k_z^2 + k_h^2}{k_z^2} \qquad \text{and} \qquad C_2 = \frac{k_z^2 - k_h^2}{k_z^2 + k_h^2}$$

We may convert these coefficients to ones that depend on a plane wave incidence angle (θ), by setting

$$\frac{v_o k_h}{\omega} = \sin\theta \quad \text{and} \quad \frac{v_o k_z}{\omega} = \cos\theta$$

Hence, C_1 and C_2 are

$$C_1 = -\frac{1}{4}\frac{1}{\cos^2\theta} \quad \text{and} \quad C_2 = \cos^2\theta - \sin^2\theta$$

This means that the reflection coefficient of the Born approximation is

$$R(\theta) = \frac{-1}{4\cos^2\theta}\left[\left(\frac{K_o}{K} - 1\right) + (\cos^2\theta - \sin^2\theta)\left(\frac{\rho_o}{\rho} - 1\right)\right] \tag{30}$$

To check equation (30) we will start with the plane wave reflection coefficient (Claerbout, FGDP, p. 173)

$$R(\theta) = \frac{\left(\rho_1 K_1 \sec^2\theta_1\right)^{1/2} - \left(\rho_2 K_2 \sec^2\theta_2\right)^{1/2}}{\left(\rho_1 K_1 \sec^2\theta_1\right)^{1/2} + \left(\rho_2 K_2 \sec^2\theta_2\right)^{1/2}} \tag{31}$$

where subscripts 1 and 2 refer to the media above and below the interface, respectively. We may generalize this to a continuous medium by putting

equation (31) in a differential form.

$$R(\theta) = \frac{\Delta z}{2} \frac{\frac{\partial}{\partial z}\left[\rho K \sec^2\theta\right]^{\frac{1}{2}}}{\left[\rho K \sec^2\theta\right]^{\frac{1}{2}}} = \frac{\Delta z}{4} \frac{\frac{\partial}{\partial z}\left[\rho K \sec^2\theta\right]}{\left[\rho K \sec^2\theta\right]} \tag{32}$$

where Δz is a frequency-dependent length scale. Using Snell's law, we substitute

$$\sec^2\theta = \left(1 - \frac{K}{\rho} p^2\right)^{-1}$$

where p is the ray parameter. Differentiating equation (32), while keeping p constant we have

$$R(\theta) = \frac{\Delta z}{4} \left[\left(\frac{\rho_z}{\rho} + \frac{K_z}{K}\right) + \frac{p^2 v^2}{1 - p^2 v^2}\left(\frac{K_z}{K} - \frac{\rho_z}{\rho}\right)\right] \tag{33}$$

Collecting terms in ρ and K we have

$$R(\theta) = \frac{\Delta z}{4\cos^2\theta}\left[\frac{K_z}{K} + (\cos^2\theta - \sin^2\theta)\frac{\rho_z}{\rho}\right] \tag{34}$$

Equation (34) has the same angle-dependence as the reflection coefficient derived from the Born approximation [equation (30)]. If we use the approximations that

$$\frac{K_o}{K} - 1 \simeq -\Delta z \frac{K_z}{K} \qquad \text{and} \qquad \frac{\rho_o}{\rho} - 1 \simeq -\Delta z \frac{\rho_z}{\rho} \tag{35}$$

then the two forms of the reflection coefficients are identical. This confirms the basic separation of modulus and density effects deduced under the Born approximation. This example also points out one of the basic restrictions of the Born approximation. The magnitude of the true reflection coefficient is never greater than unity for any value of θ. The Born reflection coefficient however, obeys no such bound. This means that the method

presented here is restricted to sub-critical reflections.

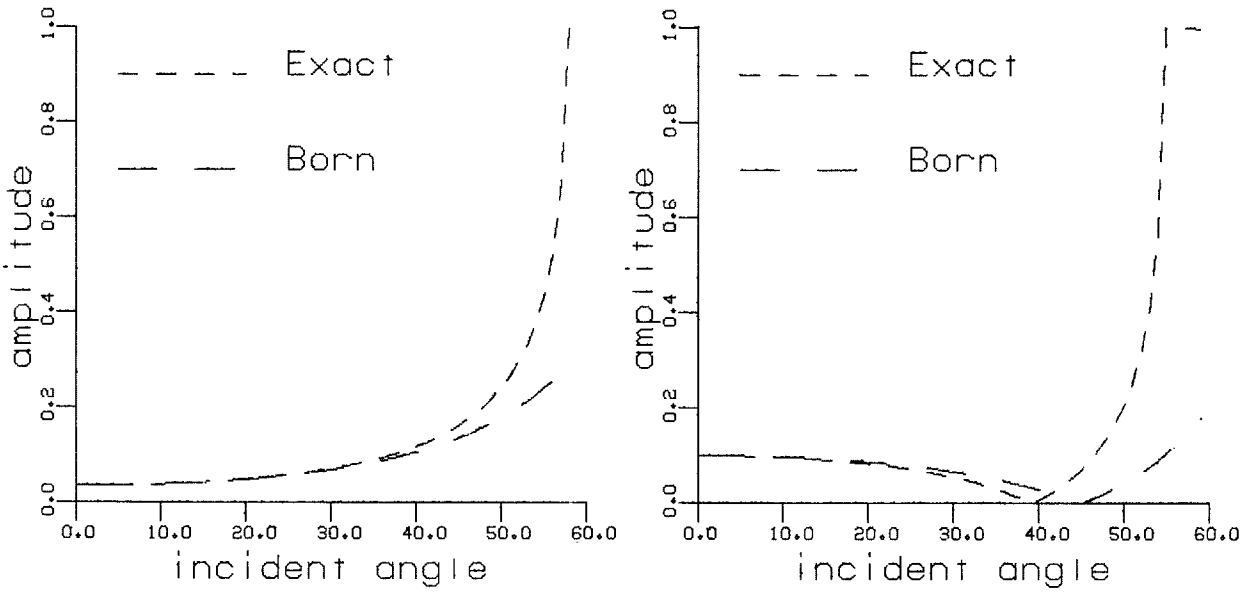

FIG. 3. A comparison of the exact reflection coefficient and the Born approximation. In the left panel, the parameter ratios are ρ_2/ρ_1 = 0.91, and K_2/K_1 = 1.27. The critical angle occurs at 58 degrees. In the right panel, the parameter ratios are ρ_2/ρ_1 = 0.67, and K_2/K_1 = 1.0, and in this case the critical angle is at 55 degrees.

A comparison of the Born reflection coefficient [equation (30)], and the exact plane wave reflection coefficient [equation (31)], is given in figure 3. The comparison is quite favorable for sub-critical angles, but towards the critical angle the two curves start to deviate. Beyond the critical angle the Born approximation completely breaks down.

VI A One-Dimensional Example

The method outlined in the previous sections was tested on a one-dimensional example. The formulas used in the inversion were basically those given in secion IV, with k_m set to zero.

In table 1, the parameters of the model are given. A synthetic gather generated by ray tracing is shown in figure 4. The synthetics include all

Layer	thickness	ρ	K	v
1	250	2.5	62.5	5.000
2	250	2.6	65.0	5.000
3	300	2.5	65.0	5.099
4	150	2.6	62.5	4.902
5	250	2.5	62.5	5.000
6	250	2.6	65.0	5.000
7	300	2.5	65.0	5.099

TABLE. 1. Parameters of the one-dimensional model.

refraction and transmission effects, as well the reflection effects of the model. The model was not specifically constructed to fit the assumptions of the Born approximation, however, a $t^{-\frac{1}{2}}$ geometric spreading factor was used to make the example two-dimensional.

In figure 5, the wave field is shown in the (k_h,k_z)-domain, after the frequency stretch [equation (19) with $k_m = 0$] has been applied. The fact that the locations of the peaks and troughs of the wave field are virtually independent of k_h means that the migration part of the algorithm has worked. The sharp cut-off in the upper part of the wave field occurs because the evanescent zone ($k_h > \omega/v$) is excluded. The summations in the least squares that follow were restricted to the non-zero part of the wave field.

The inversion of the one-dimensional example is shown in figure 6. The top three traces are the zero-offset reflectivity (r), the modulus variations (a), and the density variations (b), derived directly from the model. The next three traces were generated by filtering the top traces with a source wavelet. The bottom three traces are the results of the inversion algorithm. The reflectivity trace is a straight stack over k_h, while a and b are determined by least squares [equations (28) and (29)].

The inversion results mimic the filtered model parameters quite well, with two exceptions. First, the inverted traces are noisier, which is probably due to the finite extent of the data in the offset dimension. Presumably the application of a more sophisticated window to the data before the Fourier

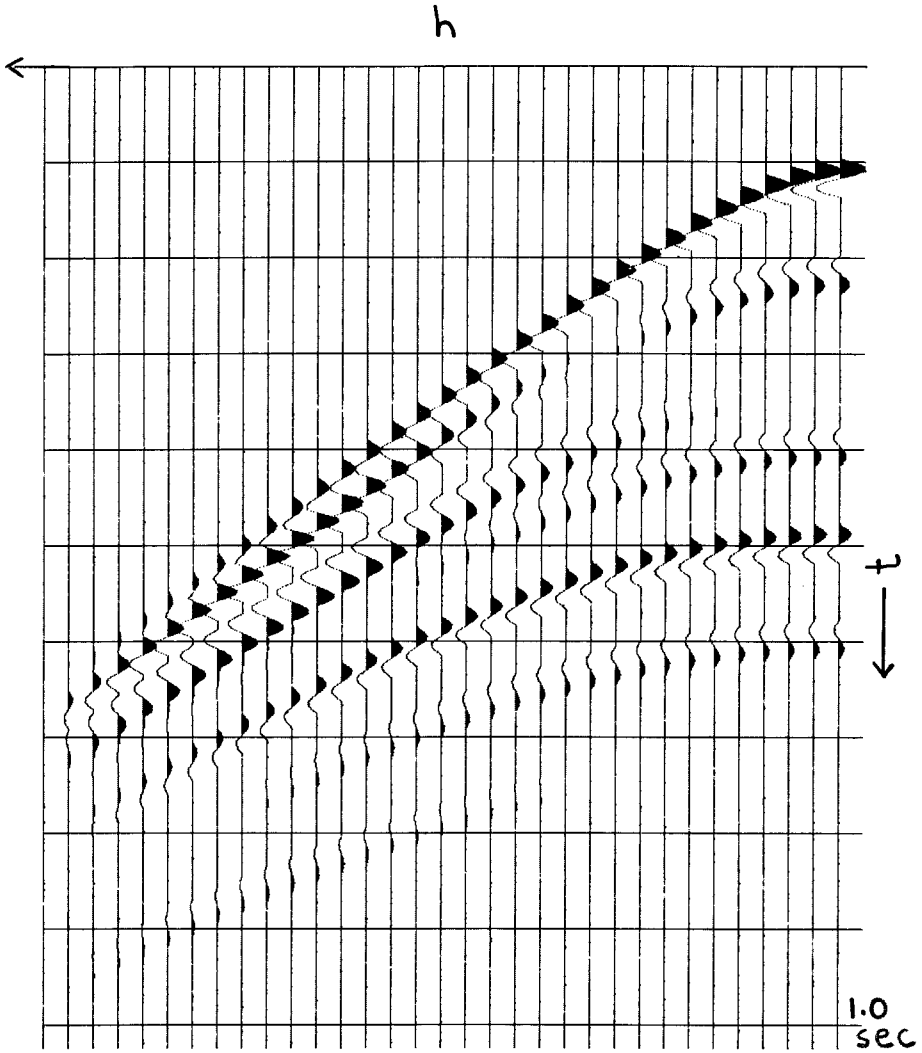

FIG. 4. A synthetic gather from a seven layer one-dimensional model. The five farthest offset traces were tapered to zero.

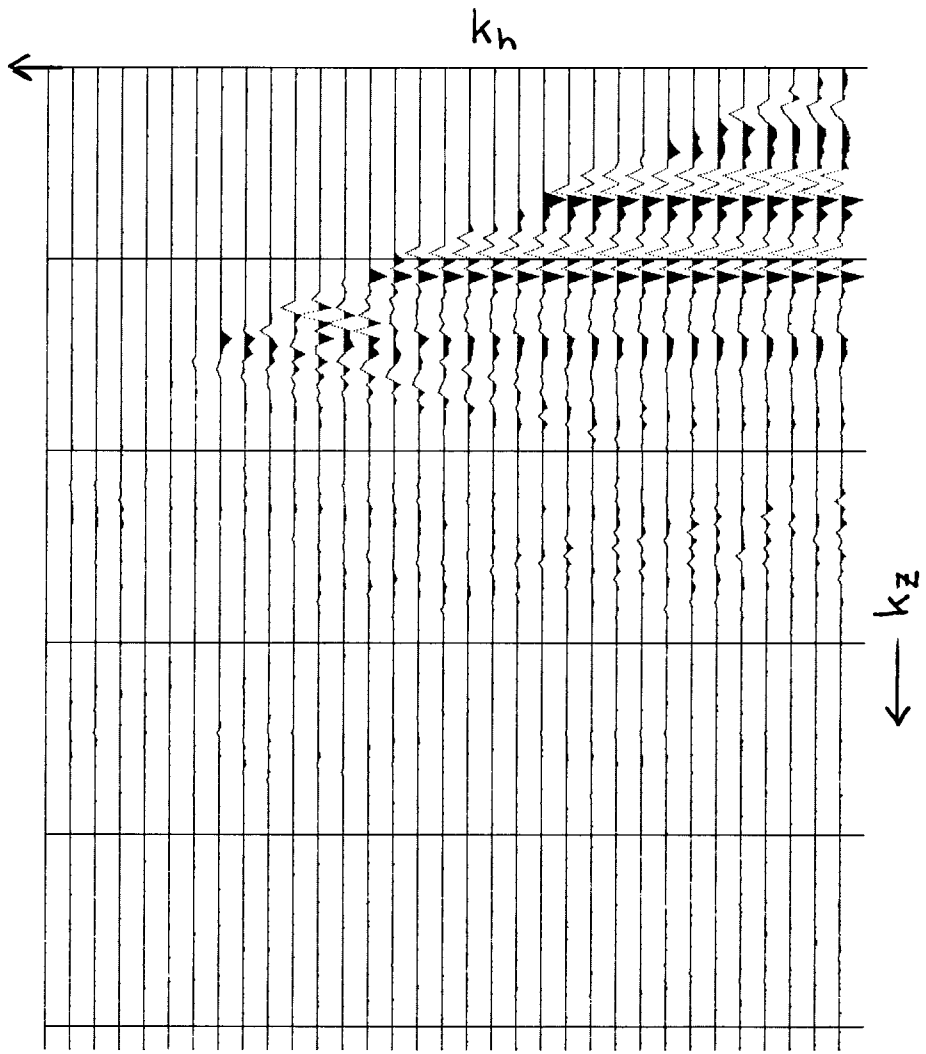

FIG. 5. The migrated wave field in the (k_h,k_z)-domain. The abrupt cutoff in the upper part of the figure is edge of the evanescent zone.

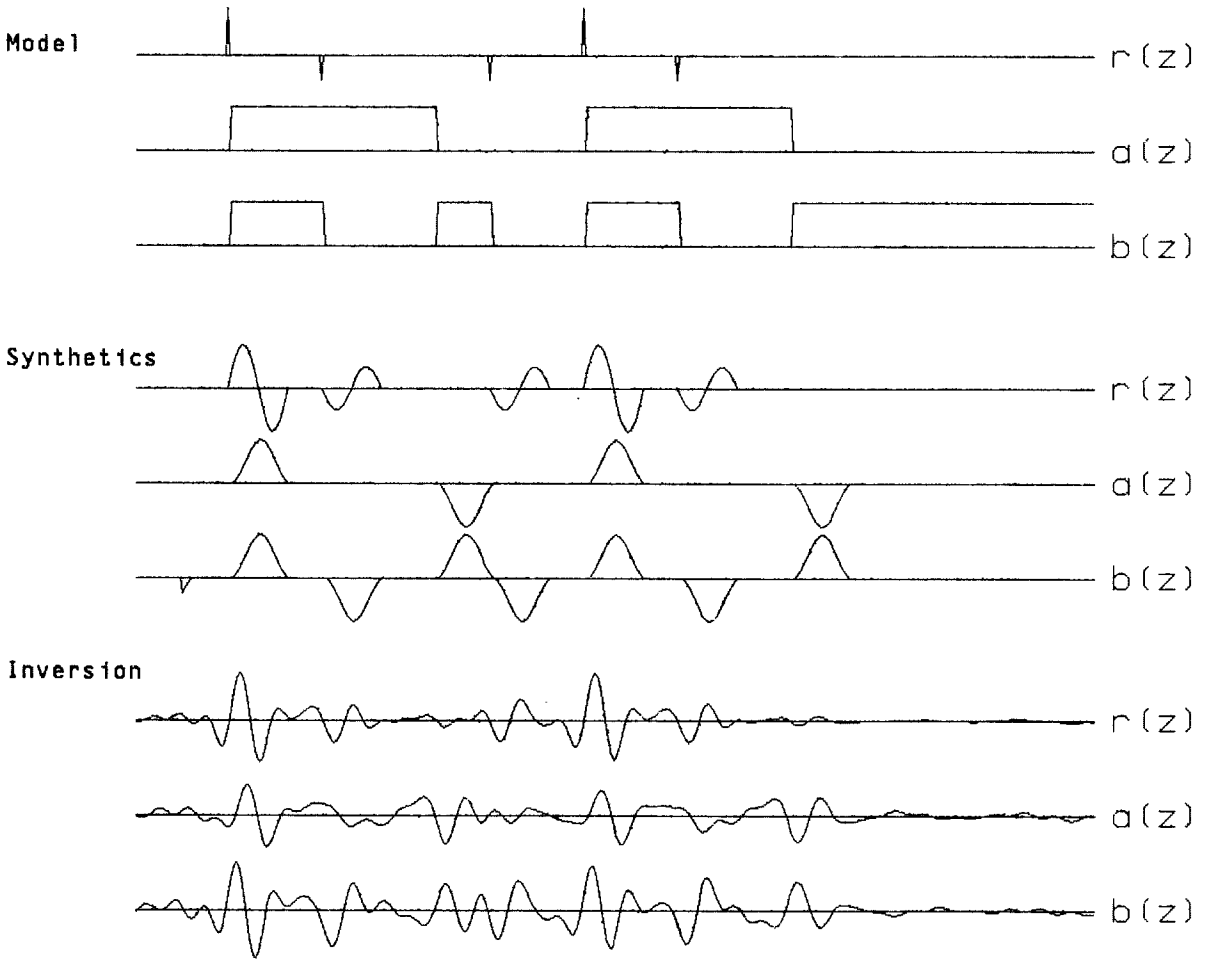

FIG. 6. Inversion results for the one-dimensional model. The top three traces are the zero-offset reflectivity (r), the modulus variations (a), and the density variations (b), determined directly from the model itself. The middle three traces filtered versions on the top three. The bottom traces are the results of the inversion.

Fourier transform would help this problem. Second, the position of some of the events is slightly off due to the fact that the Born approximation uses a constant velocity. No attempt was made in this example to deconvolve the source wavelet.

VII. A Two-Dimensional Example (in progress)

The inversion scheme was applied to data recorded in a water tank over the model shown in figure 7.[3] The words "in progress" are in the title of this section because the inversion scheme has not yet worked on this dataset. The inversion we obtain indicates that the density and modulus variations are equal in magnitude and opposite in sign. A quick examination of the model in figure 7, shows that this cannot be the case.

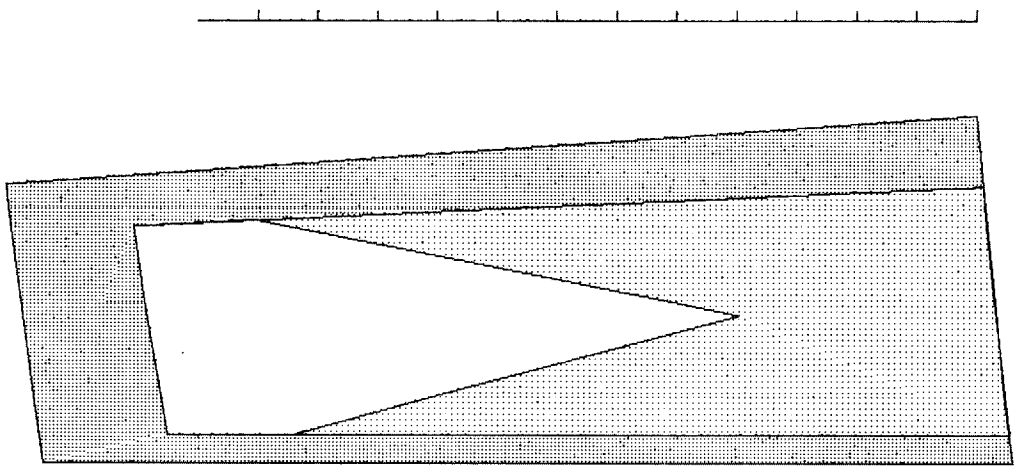

FIG. 7. The model for the two-dimensional example. The line at the top indicates the line along which the data was recorded. The white background is water with a velocity of 1525 m/sec. The light gray material has a density of 1.02 and a velocity of 1036 m/sec. The dark gray material has a density of 1.28 and a velocity of 998 m/sec.

The problem seems to lie in the fact that there is some amplitude effect that we are not accounting for. This is shown in figures 8 and 9. Figure 8 is a plot of a common-midpoint gather from the middle of the line, and shows that the amplitude variations with offset are basically smooth. Figure 9 is the $k_m = 0$ component of the migrated wave field in the (k_h, k_z)-domain. The

[3]We thank Gulf Oil Corporation for supplying us with this data.

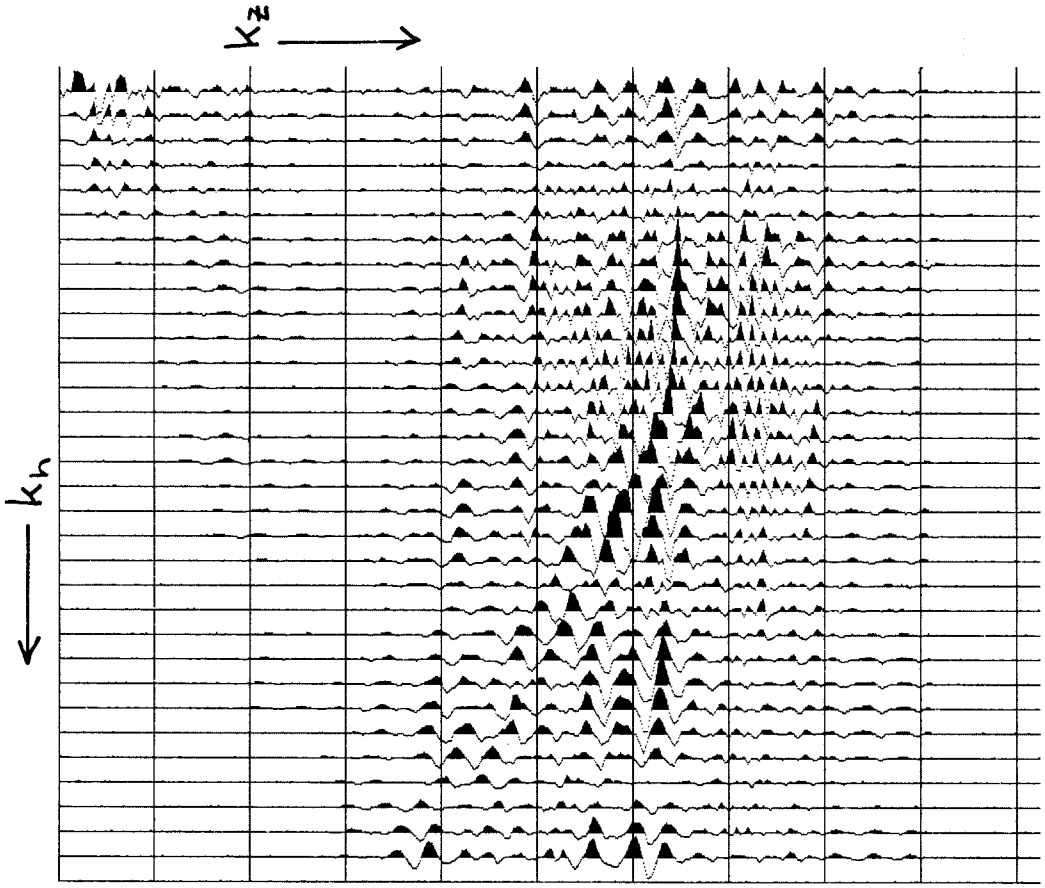

FIG. 9. The zero midpoint wavenumber component of the migrated wave field in the (k_h, k_z)-domain. The oscillatory variations in amplitude in the k_h-direction cause problems with the inversion.

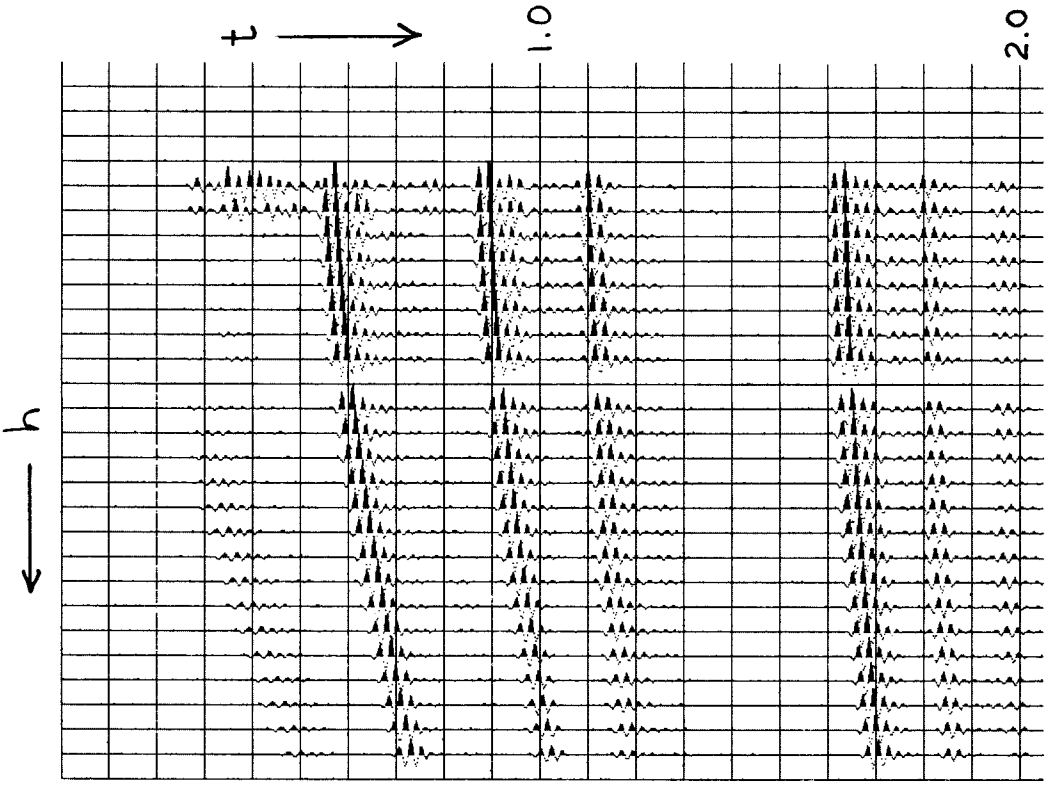

FIG. 8. A common-midpoint gather from midpoint 85. The first four offsets were not recorded, and the ninth trace is dead.

amplitude in this case oscillates with offset wavenumber. For example, there is almost a null in the wave field at the fourth offset wavenumber. It is not clear to us at this point where this variation is coming from.

APPENDIX A: The Scalar Green's Operator

The Green's operator that we will use is the one that solves the equation

$$\left(\frac{1}{\rho_0}\nabla^2 + \frac{\omega^2}{K_0}\right)\langle x|G_0|x'\rangle = -\langle x|x'\rangle \tag{A1}$$

To find G_0 we Fourier transform this equation over x

$$\left(\frac{1}{\rho_0}\mathbf{k}\cdot\mathbf{k} - \frac{\omega^2}{K_0}\right)\langle k|G_0|x'\rangle = \frac{1}{2\pi}e^{i\mathbf{k}\cdot x'} \tag{A2}$$

where k is the dual of x, and has components (k_x,k_z). In the two-dimensional problem (line sources and receivers), x and k_x are scalars. The equations that follow will hold for the three-dimensional problem if we consider x and k_x to be two component vectors, and adjust the occasional factor of 2π. The sign convention of the Fourier transform that we use in this paper is

$$\langle x,t|\omega,k\rangle = e^{-i\omega t + \mathbf{k}\cdot x}$$

Solving for G_0 in equation (A2) we have

$$\langle k_x,k_z|G_0|x',z'\rangle = \frac{\rho_0}{2\pi}\frac{e^{ik_x x' + ik_z z'}}{(k_z-\nu)(k_z+\nu)} \tag{A3}$$

where

$$\nu = \left(\frac{\omega^2}{v_0^2} - k_x^2\right)^{1/2} \quad \text{and} \quad v_0^2 = \frac{K_0}{\rho_0}$$

The domain in which we will use the Green's operator will be the (k_x,z)-domain. To find the Green's operator in this domain we inverse transform over k_z.

$$\langle k_x,z|G_o|x',z'\rangle = \frac{\rho_o}{(2\pi)^{3/2}} \int dk_z \frac{e^{ik_x x' + ik_z(z'-z)}}{(k_z - \nu)(k_z + \nu)} \qquad (A4)$$

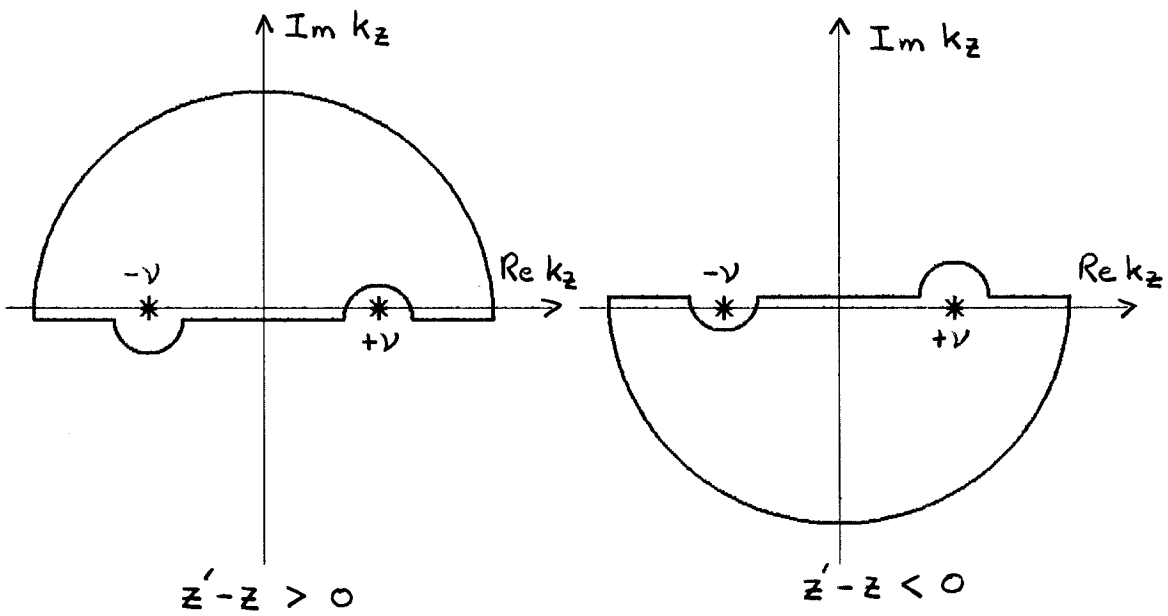

FIG. 10. The integration contour for the Green's operator is shown for two cases

The transform is evaluated by contour integration in the complex k_z-domain. The contours are shown in figure 10. Two considerations affect the choice of contour path. The first is that we want the exploding Green's operator, which means we only want to include the contribution of one of the poles. The appropriate pole is the one which makes $k_z(z'-z) \leq 0$. Second, we need to preserve the radiation condition that the field goes to zero as z goes to infinity. For $(z'-z) > 0$ the contour is closed in the upper half-plane and the pole at $k_z = -\nu$ is included. When $(z'-z) < 0$, the contour is closed in the lower half-plane and the pole at $k_z = +\nu$ is enclosed.

Using the residue theorem the Green's operator is found to be

$$\langle k_x, z|G_0|x', z'\rangle = \langle k_x|x\rangle \langle x, z|G_0|x', z'\rangle = i\frac{\rho_0}{(2\pi)^{\frac{1}{2}}} \frac{e^{ik_x x' - i\nu|z'-z|}}{-2\nu} \quad (A5)$$

To find the form of the exploding Green's operator when transformed over the initial set of states we simply forward transform over k_x and inverse transform over x'. The result is

$$\langle x', z'|G_0|k_x, z\rangle = \langle x', z'|G_0|x, z\rangle \langle x|k_x\rangle = i\frac{\rho_0}{(2\pi)^{\frac{1}{2}}} \frac{e^{-ik_x x' - i\nu|z'-z|}}{-2\nu} \quad (A6)$$

APPENDIX B: The Fourier Transform of the Scattering Potential

If the scattering potential is local (b=0 in the present formulation), then its Fourier transform would be trivial to compute. In the general acoustic problem, the potential is non-local because it contains spatial derivatives, which means we have to exercise a little more care in finding its Fourier transform.

An equivalent form for writing the scattering potential is

$$V(x'|x'') = (\omega^2 \frac{a(x')}{K_0} + \nabla \cdot \frac{b(x')}{\rho_0} \nabla) \delta(x'-x'') \quad (B1)$$

We now Fourier transform over x' and x''.

$$V(k'|k'') = (2\pi)^{-2} \int dx' \int dx'' e^{ik'\cdot x'} (\omega^2 \frac{a(x')}{K_0} + \nabla \cdot \frac{b(x')}{\rho_0} \nabla) \delta(x'-x'') e^{-ik''\cdot x''}$$

First we integrate over x'' to obtain

$$V(k'|k'') = (2\pi)^{-2} \left[\int dx' \, e^{i(k' - k'')\cdot x'} \, \omega^2 \frac{a(x')}{K_0} + \int dx' \, e^{ik'\cdot x'} \nabla \cdot \frac{b(x')}{\rho_0} \nabla e^{-ik''\cdot x'} \right]$$

In the second integral we integrate by parts ($\int u\, dv = uv| - \int v\, du$) with

$$u = e^{ik'\cdot x'} \quad \text{and} \quad dv = \nabla\cdot\frac{b}{\rho_o}\nabla e^{-ik''\cdot x'}$$

This changes the second integral to

$$-\int dx'\left[\nabla e^{ik'\cdot x'}\right]\frac{b(x')}{\rho_o}\left[\nabla e^{-ik''\cdot x'}\right]$$

Combining the first and second parts of the integral, the Fourier transform of the scattering potential is

$$V(k'|k'') = (2\pi)^{-2}\left[\omega^2\,\frac{a(k'-k'')}{K_o} - k'\cdot k''\frac{b(k'-k'')}{\rho_o}\right] \qquad (B2)$$

The medium parameters (a and b) are functions only of the difference of the two wavenumbers ($k' - k''$).